Hindawi
Geofluids
Volume 2022, Article ID 6198660, 13 pages
https://doi.org/10.1155/2022/6198660

Research Article

Fuzzy Random Prediction Model of Frost Heave Characteristics of Horizontal Frozen Metro Contact Channel in Coastal Area

Yao Yafeng[1,2] **Zhang Zhemei,**[3] **Wang Wei,**[1] **Li Yongheng,**[1] **Li Siqi,**[1] **and Wei Chenguang**[4]

[1]*School of Architectural Engineering, Nantong Vocational University, Nantong 226001, China*
[2]*Department of Civil Engineering, Anhui Jianzhu University, Hefei 230601, China*
[3]*College of Civil Engineering, Tongzhou Secondary Vocational School, Nantong 226399, China*
[4]*Zhiju Prefabricated Green Building Innovation Center Nantong Co., LTD., Nantong 226001, China*

Correspondence should be addressed to Yao Yafeng; mike.yyf@yeah.net

Received 5 December 2021; Revised 28 January 2022; Accepted 18 February 2022; Published 17 March 2022

Academic Editor: Dongdong Ma

The frost heave characteristics of artificial frozen soil are very important information for underground freezing engineering. It is found that both the frost heaving force and rate of the same soil layer increase with the decrease of freezing temperature. In addition, due to the comprehensive influence of freezing temperature, natural water content, dry density, and tidal flow peak value, the frost heave characteristics of different soil samples are evidently uncertain. With the aim of improving the deficiency of traditional BP neural network algorithms in solving fuzzy random engineering problems, random factor and mean square error between layers are used to modify the evaluation function of the network model. On this basis, taking tidal flow peak value, freezing temperature, natural water content, and dry density as inputs, the frost heaving force and rate of frozen soil as output values, and setting the number of hidden layer elements as 4, an improved fuzzy random BP network prediction model for frost heave characteristics was established. The new network prediction model has a smaller weight and bias, and the response tends to be smoother than the traditional one, which greatly reduces the overfitting phenomenon. The engineering example shows that the improved BP neural network prediction model can make the predicted value of frost heaving force and rate basically coincide with the measured value after effective training, and the error is controlled within 8%. Therefore, the prediction model can be used as an effective tool to predict frost heaving characteristics in Nantong metro freezing construction, and the corresponding model and method can also be extended to similar engineering cases.

1. Introduction

With the rapid development of urbanization, metro construction has been in full swing in many cities to solve the problem of urban traffic congestion. During the process of metro excavation, the contact passage that connects the up and down tunnels not only ensures the safe evacuation of passengers but also plays the role of water collection and drainage between stations during metro operation. Therefore, the construction risks of the contact passage and the corresponding measures have attracted more and more attention. The artificial freezing method has many advantages such as strong structural adaptability, no environmental pollution, and good water insulation, and it is often used in the construction of metro contact passages [1, 2].

Nantong belongs to the delta alluvial plain landform of the lower reaches of the Yangtze River. The overall soil quality is relatively soft, with high water content, large hydraulic slope, and obvious tidal flow in different seasons. Based on the complex hydrogeological conditions in Nantong, the frost heave characteristics of soil caused by the phase change of ice water are obviously uncertain as the temperature decreases during the freezing construction of the metro contact passage. This often leads to uneven random deformation around the tunnel, which is unfavorable to the existing contact passage and even affects the construction safety of the

Table 1: Main physical parameters of clay layers.

Soil sample	Depth (m)	Tidal flow peak value (cm)	Moisture content (%)	Dry density (g/cm^3)	Plastic index
1	9.6	55	20.91	1.62	12.0
2	12.1	129	23.42	1.54	12.7
3	15.0	82	21.48	1.60	11.9
4	18.6	167	23.14	1.56	12.5

Figure 1: Clay sample specimen.

whole metro project. Therefore, it is of great practical significance to study the characteristics of horizontal frost heaving in the freezing construction process of connecting passage of the metro in a coastal area for tunnel construction safety of Nantong metro.

Scholars at home and abroad have done much research and discussion on the frost heave characteristics. Jihui et al. [3] analyzed the frost heaving degree of frozen soil in different frozen regions by numerical calculation and then deduced theoretical analytical solutions of the frost heaving force according to the distribution of frost heaving loads. Lu et al. [4] took fractured sandstone as the research object and carried out a frost heaving cycle test. On this basis, the uniaxial compressive strength damage prediction model was established by comprehensively considering cracks, confining pressure, and other factors, and the accuracy of the model was verified through engineering cases. Lu et al. [5] carried out frost heaving tests under different confining pressures, deviatoric stresses, temperature gradients, and water supply conditions. Based on the Takashi one-dimensional frost heaving rate model, an improved prediction model for saturated cohesive soil frost heaving rate was established considering the effects of stress level and temperature gradient. Zhu et al. [6] determined the stress field and displacement field according to the continuous conditions of tunnel lining, frost heaving region, and unfrozen surrounding rock and established a new analytical solution. On this basis, the analytical solution was verified by taking the Zhegushan tunnel as an example. Zhou et al. [7] used the multilayer field test and separation potential model to calculate the temperature gradient and bimodal function according to the field monitoring results and proposed a simplified frost heave prediction method based on the concept of separation potential. Liu et al. [8] established a fully coupled model of frozen soil frost heave, temperature distribution, and pore water pressure under the framework of poroelasticity theory and porosity function. Luo et al. [9] conducted a series of freezing temperature and freezing tests on unsaturated expansive clay. The results show that the swelling amount of expansive clay is the displacement and frost heave caused by the increase of water content in the unfrozen region. It is found that the state and change of pore water are the key factors determining the frost heave characteristics of unsaturated expansive clay in the open system.

To sum up, previous studies on horizontal frost heave characteristics of artificial frozen soil were mostly based on experimental data analysis and formula calculation, without considering the influence of tidal flow on frost heave. Engineering practice shows that under the comprehensive action of tidal flow, temperature, lithology, and other factors, the frost heave characteristics in underground freezing engineering have obvious uncertain distribution. Therefore, the characteristics of frost heave in underground engineering cannot be accurately characterized only by traditional empirical formulas and experimental data analysis.

Therefore, based on the frost heaving test of clay layer in Nantong under tidal flow, the improved BP neural network is used to predict the horizontal frost heaving characteristics of the metro contact passage during freezing construction in view of the uncertainty of permafrost parameter distribution. It is expected that the frost heave data obtained can effectively prevent the underground tunnel location deviation and section damage and provide effective basic data for the underground freezing engineering in Nantong and its surrounding areas.

2. Frost Heaving Test of Soil Samples

2.1. Soil Sample Making. The underground tunnel of Nantong metro line 1 has a total length of 34.75 km with 25 stations, and contact passages between stations along the line were constructed by the freezing method. To ensure the engineering representativeness of frost heaving test results, the undisturbed soil was collected from the horizontal frozen clay layer of Nantong metro under the action of tidal flow. The physical parameters of each soil sample are shown in Table 1. The collected soil samples were carefully packed and sealed with double-layer plastic fresh-keeping bags, recorded, and tied with ropes. The bundled soil samples were then loaded into sampling cylinders, labeled, sealed with adhesive tape, loaded into the core box, and safely transported to the laboratory [10]. The core box was carefully opened, and the soil samples were divided into upper and lower layers according to natural deposition direction, and both ends were sawed flat. According to the Chinese Artificial Frozen Soil Test Standard (MT/T593.6-2011), the sawed soil samples were made into $\Phi 50 \times 100$ mm specimens, the shape error was within 1.0%, and the parallelism

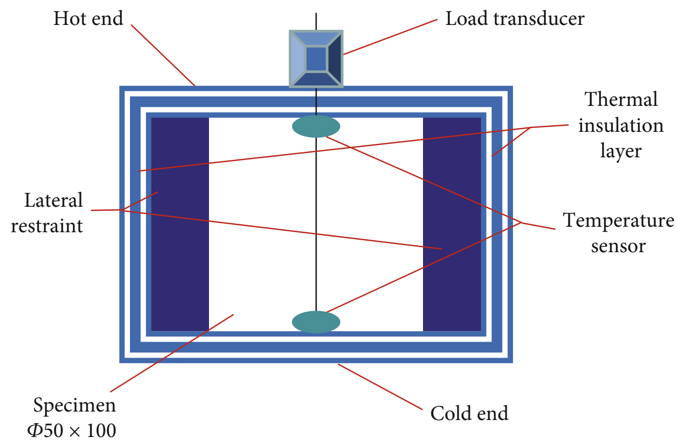

FIGURE 2: Diagram of freezing heave test device.

TABLE 2: Maximum frost heaving rate and frost heaving force of different soil samples.

Soil sample	Frost heaving force (MPa)			Rate of frost heave (%)		
	-5°C	-10°C	-15°C	-5°C	-10°C	-15°C
1	0.33	0.40	0.46	2.34	3.26	3.97
2	0.48	0.54	0.62	3.91	4.59	5.34
3	0.36	0.42	0.53	2.45	3.16	3.92
4	0.43	0.49	0.57	3.64	4.28	4.83

error was within 0.5 mm. The standard specimen of a prepared clay sample is shown in Figure 1.

2.2. Frost Heaving Test. Per MT/T593.2-2011, the cold end temperature of the frost heaving instrument was adjusted to the test temperature, and the error was controlled within 0.2°C. The prepared soil sample was placed into the low-temperature cabinet to control the freezing temperature in the test process, and the film was wrapped around the specimen for effective insulation. When the temperature of the cold end equaled the test temperature, the specimen was loaded and the two ends lightly pressed to ensure that the specimen was in good contact with the test device and could expand freely in the axial direction. The displacement sensor was installed and debugged, the real-time data acquisition system was opened, and the height change value of the specimen was recorded by intervals of 1 min, 2 min, 5 min, 10 min, 20 min, 30 min, 1 h, 2 h, 3 h, 6 h, 12 h, and 14 h. During the test, the axial frost heaving amount was recorded according to the reading of displacement meter, and the ratio of it to the original size of specimen was the frost heaving rate [11]. In addition, the displacement meter was replaced with a load sensor. When a sample did not continue to freeze heave at an interval of 2 h after loading a certain level of load (frost heave ≤ 0.01 mm), the sample was considered stable under this level of load, and the frost heaving force at this moment was recorded [12]. The frost heaving test device is shown in Figure 2.

According to the above test method and steps [13], frost heave characteristics tests were conducted at -5, -10, and -15°C, respectively. The results of maximum frost heaving rate and maximum frost heaving force of different soil samples are shown in Table 2.

The frost heaving curves of different soil samples with time were collected by computer in real time [14, 15], as shown in Figure 3. Curves of frost heaving rate with time at all temperatures are shown in Figure 4.

During the frost heaving force tests, the axial frost heaves were recorded according to the reading of the displacement meter [16]. The ratio of the axial frost heave to the original size of the specimen is the frost heaving rate, as shown in

$$\eta = \frac{\delta}{H} \times 100\%, \tag{1}$$

where η is the frost heaving rate, δ is the axial frost heave, and H is the original size of the specimen.

According to the frost heaving tests, it is found that under the action of tidal current, the frost heaving force of frozen clay in Nantong metro is between 0.33 and 0.62 MPa, and the corresponding frost heaving rate is between 2.34% and 5.34%. By observing the frost heaving curves, it can be seen that in general, the frost heaving force and rate of the same soil layer increase with the decrease of freezing temperature. In addition, due to the comprehensive influence of freezing temperature, natural water content, dry density, tidal current peak, and other parameters, the frost heaving characteristics of different soil samples show obvious uncertainty.

Therefore, in the complex environment, in order to master the frost heaving law of freezing engineering more effectively, artificial intelligence algorithms and appropriate improvement are needed to help us predict the frost heaving characteristics of frozen soil more accurately.

3. BP Neural Network and Its Improvement

3.1. BP Neural Network. In 1986, the scientist Ruml Hart proposed the error backpropagation intelligent algorithm

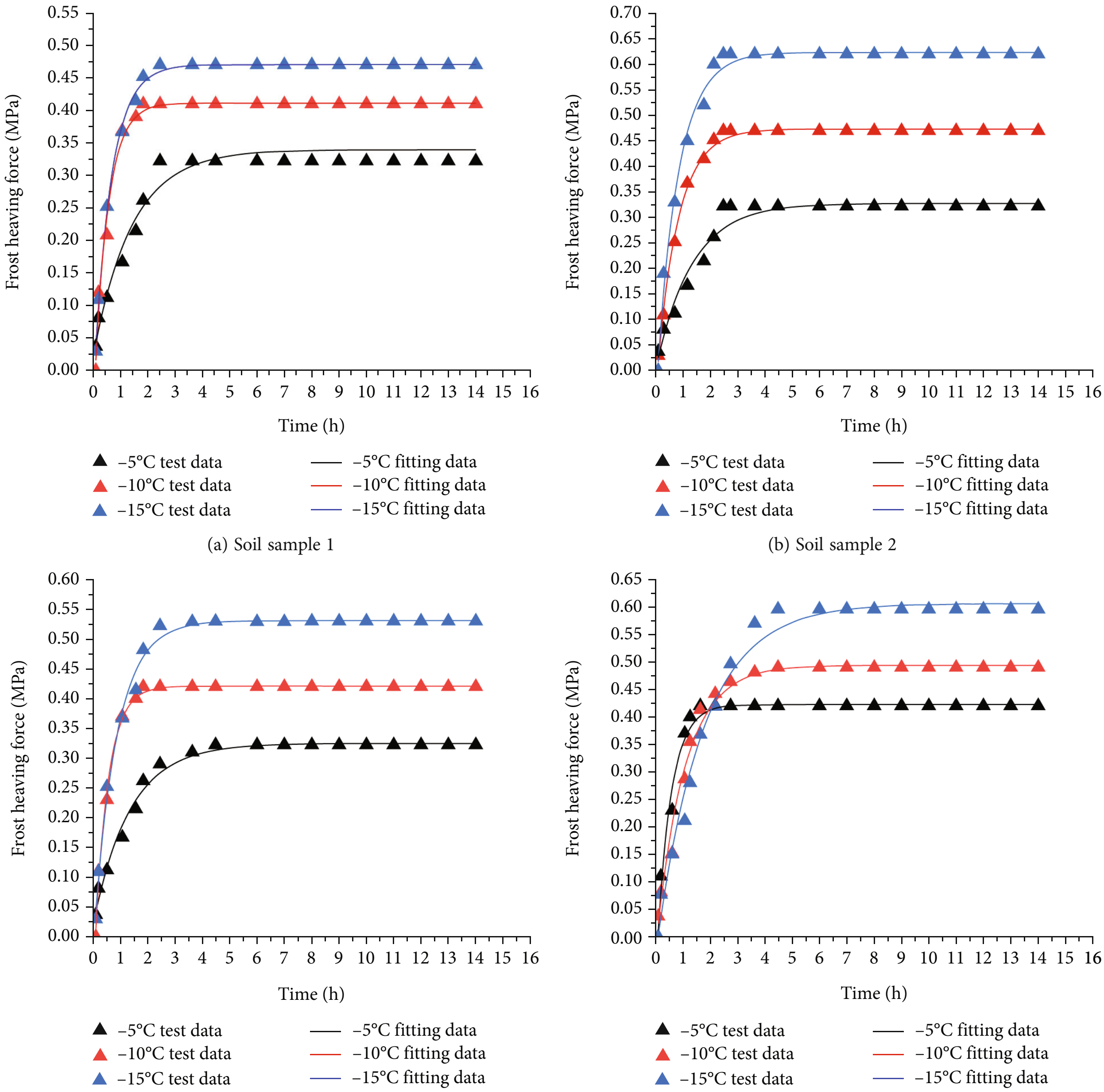

(a) Soil sample 1

(b) Soil sample 2

(c) Soil sample 3

(d) Soil sample 4

Figure 3: Relation curve between frost heaving force and time.

(BP algorithm), which solved the problem of learning the connection weights between hidden layer elements in multilayer neural networks through the forward circulation of information elements and the feedback transmission of error elements and established the BP neural network model [17, 18]. The network topology of the model consists of input, intermediate, and output, as shown in Figure 5. The information flow of the model is divided into positive flow and negative feedback. In the initial operation, the information flows in the traditional order of input layer ⟶ hidden layer ⟶ output layer. If there is an error between the output value and the expected value, the negative feedback propagation is started. The error signal is returned along the original neurons, and the weights of neurons in each layer are modified so that the iteration is repeated until the error disappears or is within the allowable range [19, 20].

The algorithm steps of BP neural network as shown in Figure 4 are as follows [21, 22]:

(1) Random initialization of connection weights

$$\omega_{sp} = \mathrm{Random}(\cdot), \tag{2}$$

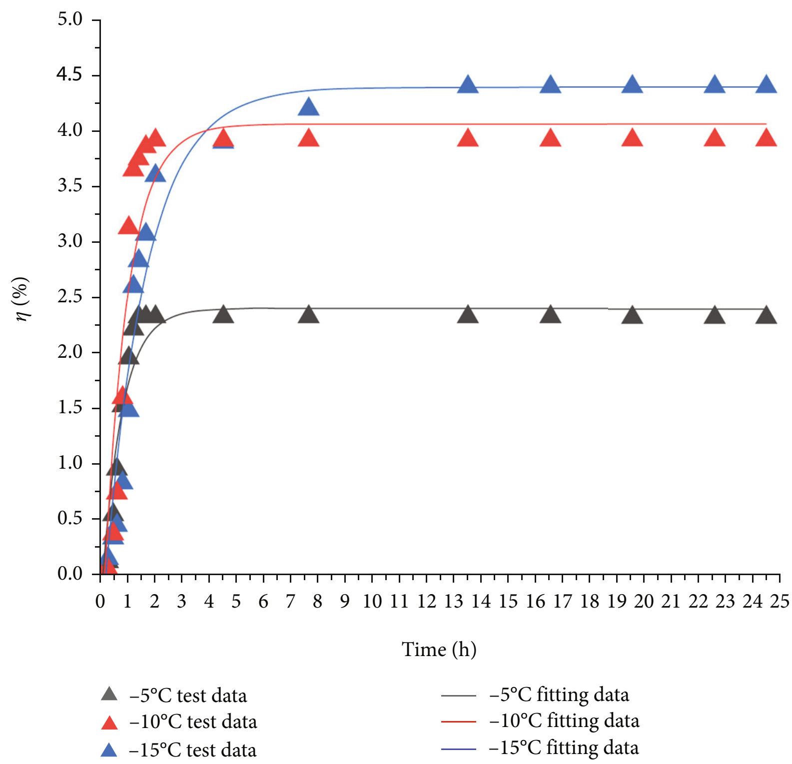

(a) Soil sample 1

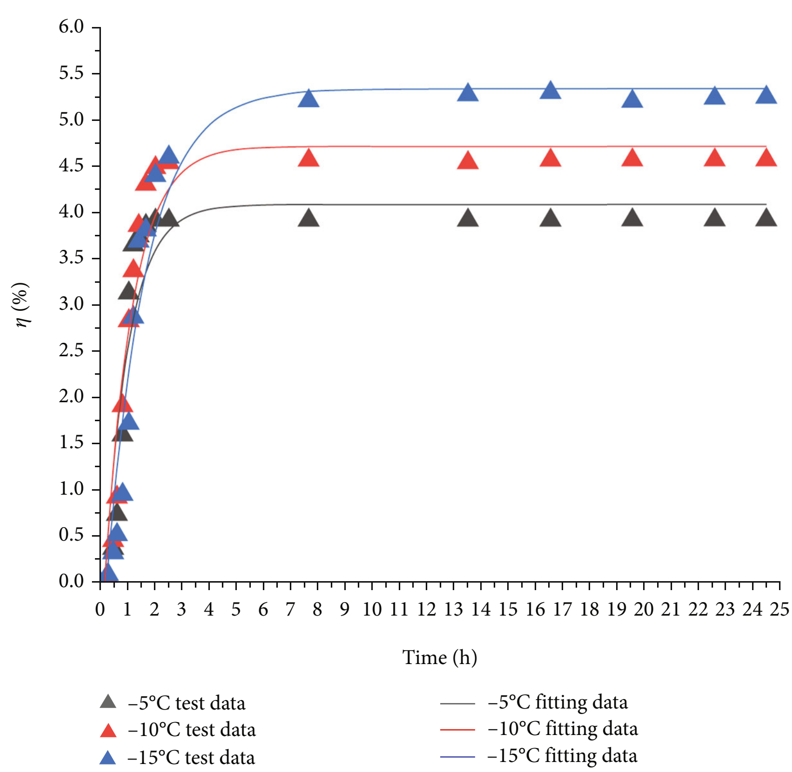

(b) Soil sample 2

Figure 4: Continued.

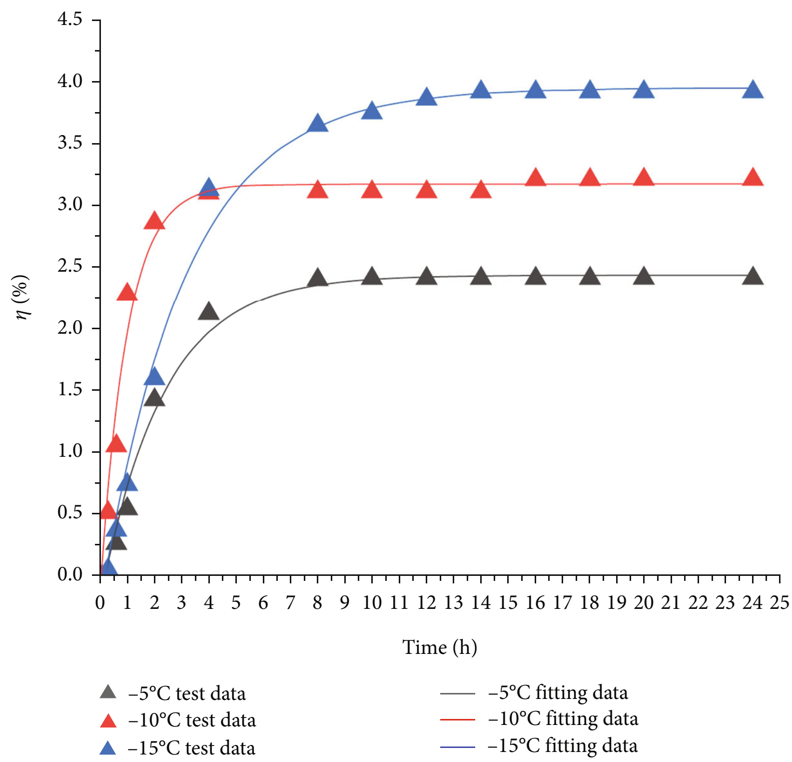

(c) Soil sample 3

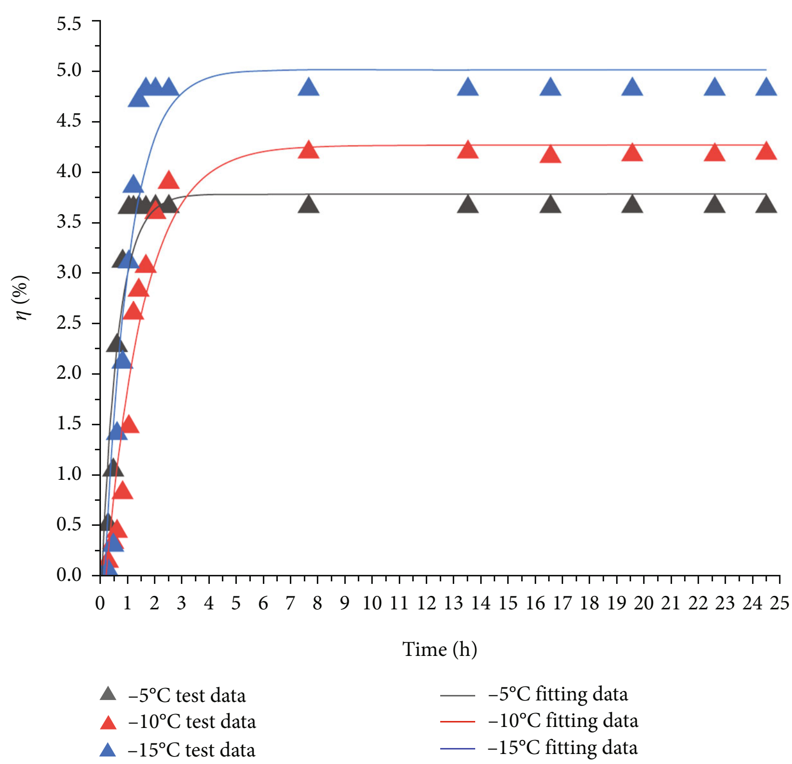

(d) Soil sample 4

Figure 4: Relation curve between frost heaving rate and time.

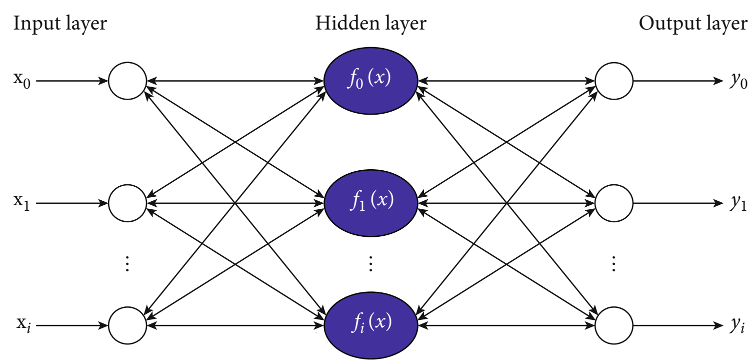

FIGURE 5: BP neural network.

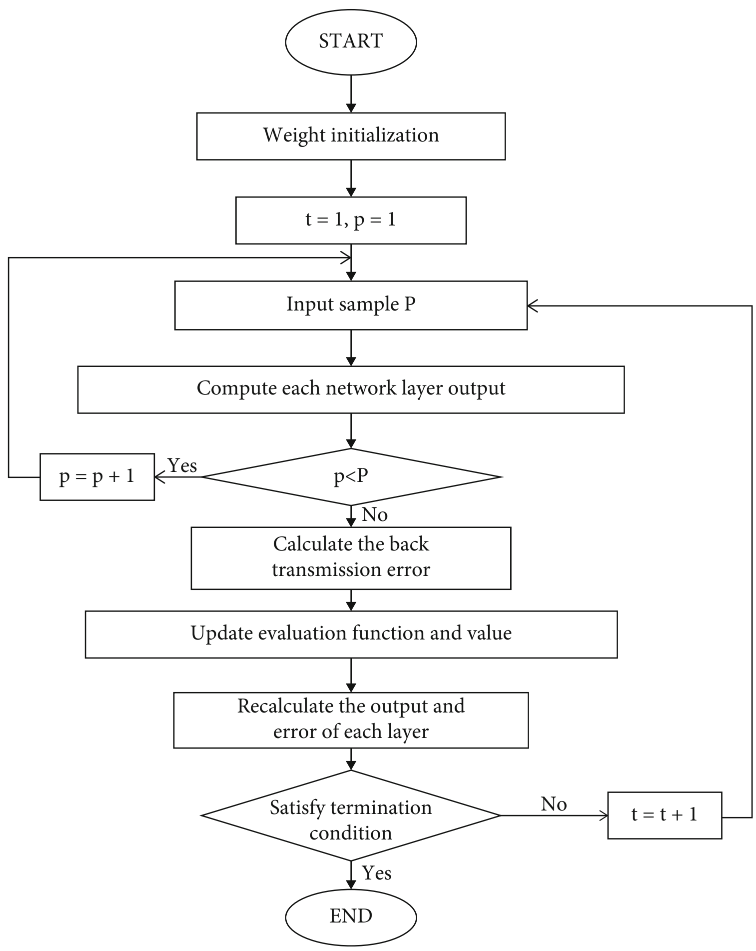

FIGURE 6: Improved BP network algorithm flow.

where s and p are different nodes of network neurons, ω is the corresponding node connection weight, and Random() is the random number generator

(2) According to the network model, P samples are input to promote network learning in turn, and the input serial number of the current sample is assumed to be P

(3) Calculate the signal output of each layer in turn by Sigmoid function: $f_0(x), f_1(x), f_i(x), \cdots, y_0, y_1, y_i$

(4) Calculate the feedback error of each layer, respectively

$$\delta_{kl}^{(p)} = \left(d_l^{(p)} - y_l^{(p)}\right) y_l^{(p)} \left(1 - y_l^{(p)}\right), \tag{3}$$

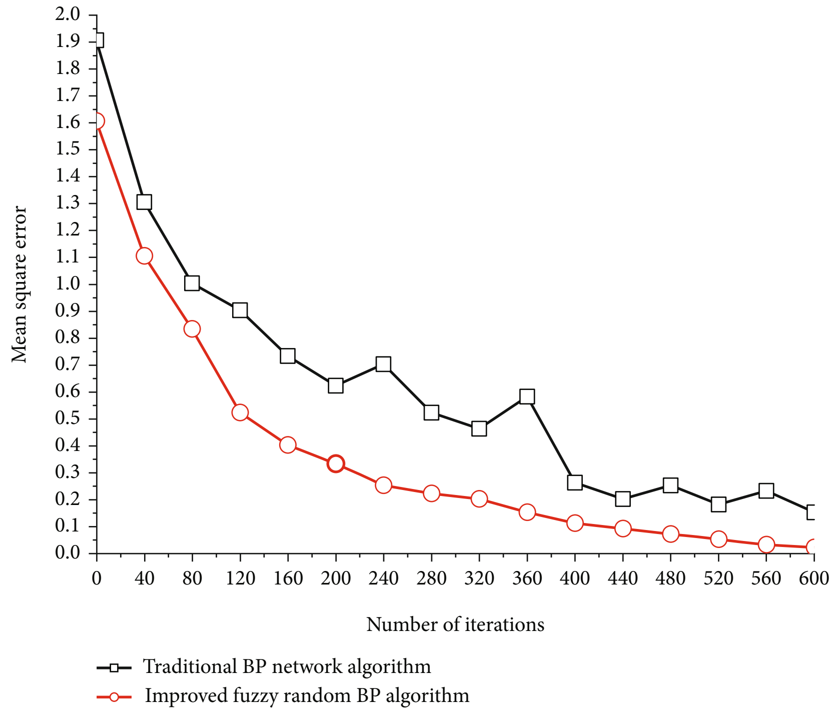

Figure 7: Efficiency comparison between the traditional and improved algorithms.

where $l = 0, 1, 2, \cdots, m-1$,

$$\delta_{\mathrm{jk}}^{(p)} = \sum_{l=0}^{m-1} \delta_{\mathrm{kl}}^{(p)} \omega''_{kl} x''^{(p)}_{k} \left(1 - x''^{(p)}_{k}\right), \tag{4}$$

where $k = 0, 1, 2, \cdots, n_2$,

$$\delta_{\mathrm{ij}}^{(p)} = \sum_{k=0}^{n_2} \delta_{\mathrm{jk}}^{(p)} \omega'_{jk} x'^{(p)}_{j} \left(1 - x'^{(p)}_{j}\right), \tag{5}$$

where $j = 0, 1, 2, \cdots, n_1$

Write down the values of$x''^{(p)}_{k}$, $x'^{(p)}_{j}$, and $x_i^{(p)}$ when transmitting feedback signals.

(5) Judge whether the current number of learning samples meets the requirements. When $p < P$, the iterative learning continues, and the algorithm goes to step (2); if $p = P$, the iterative learning ends, and the algorithm jumps to step (6)

(6) Recalculate the connection weights of network nodes according to the weight correction formula

(7) According to the modified weights, calculate x'_i, ϵ, and y_l; if each p and l can make $|d_l^{(p)} - y_l^{(p)}| < \varepsilon$ or reach the maximum learning times, then the algorithm ends and the result is output. Otherwise, go to step (2) to continue the iterative calculation

3.2. Fuzzy Random Improvement of BP Network. Although BP neural network algorithm is widely used in engineering, it is found in practice that the algorithm has obvious shortcomings in the analysis of randomness problems, especially the selection of evaluation function has a great influence on the network performance, which may lead to the overfitting phenomenon of the network and make the inaccurate output results of BP model. Therefore, the following improvements were adopted to address the shortcomings of evaluation functions in the traditional algorithm [23, 24].

$$\operatorname{Re} g = \gamma \mathrm{mse} + (1-\gamma)\mathrm{msw}, \tag{6}$$

where $\gamma \in [0, 1]$ is a random correction factor and mse is the mean square error between network layers, as shown in

$$\mathrm{mse} = \frac{1}{P} \sum_{n=1}^{P} \frac{\left(d^{(p)} - y^{(p)}\right)^2}{2}, \tag{7}$$

where msw is the weight of the network layer, and the fuzzy membership function can be determined according to the following methods:

$$\begin{aligned} \mathrm{msw}_1 &= \frac{1}{N_\omega} \sum_{i=1}^{N_\omega} (\omega_i)^2, \\ \mathrm{msw}_2 &= \frac{1}{N_\omega} \sum_{i=1}^{N_\omega} |\omega_i|, \\ \mathrm{msw}_3 &= \frac{1}{N_\omega} \frac{1}{\alpha} \sum_{i=1}^{N_\omega} \lg\left(1 + \alpha^2 {\omega_i}^2\right), \end{aligned} \tag{8}$$

Table 3: Training results of the prediction model.

Serial number	Input parameters: Tidal flow peak value (cm)	Freezing temperature (°C)	Moisture content (%)	Dry density (g/cm^3)	Output value and error: Frost heaving force (MPa)	Error of frost heaving force (%)	Frost heaving rate (%)	Error of frost heave rate (%)
1	78	-5	22.43	1.70	0.33	-7.92	4.33	6.40
2	82	-10	22.43	1.70	0.45	-4.97	3.70	-4.94
3	117	-15	22.43	1.70	0.56	7.59	5.49	5.75
4	85	-5	22.43	1.65	0.41	3.43	3.51	-4.06
5	195	-10	22.43	1.65	0.52	-7.76	4.25	7.62
6	154	-15	22.43	1.65	0.68	4.77	5.03	-6.36
7	104	-5	26.17	1.46	0.39	5.88	5.23	5.06
8	128	-10	26.17	1.46	0.54	-5.74	5.04	-4.63
9	217	-15	26.17	1.46	0.63	-4.35	5.86	-2.48
10	98	-5	26.17	1.53	0.43	7.57	4.75	4.40
11	174	-10	26.17	1.53	0.48	5.17	5.15	-6.73
12	257	-15	26.17	1.53	0.59	3.01	6.07	-4.20
13	148	-5	19.33	1.76	0.42	-4.53	2.81	2.95
14	96	-10	19.33	1.76	0.51	5.36	3.50	3.08
15	157	-15	19.33	1.76	0.66	-6.94	4.43	-8.54
16	111	-5	19.33	1.72	0.39	7.82	3.03	-3.95
17	96	-10	19.33	1.72	0.48	-5.02	3.74	-2.86
18	177	-15	19.33	1.72	0.56	-2.66	4.18	4.64
19	56	-5	17.06	1.80	0.32	7.10	3.23	5.70
20	173	-10	17.06	1.80	0.40	8.57	4.01	6.26
21	231	-15	17.06	1.80	0.53	-6.15	4.61	-4.63
22	84	-5	17.06	1.84	0.46	3.22	3.43	5.68
23	137	-10	17.06	1.84	0.53	-6.47	4.84	-3.20
24	195	-15	17.06	1.84	0.66	7.59	5.06	-3.13
25	79	-5	24.52	1.51	0.43	4.06	3.09	5.40
26	143	-10	24.52	1.51	0.50	5.05	3.42	4.15
27	190	-15	24.52	1.51	0.58	5.44	4.69	6.40
28	127	-5	24.52	1.43	0.39	-6.74	3.84	7.34
29	103	-10	24.52	1.43	0.44	-5.35	3.03	2.75
30	195	-15	24.52	1.43	0.52	7.57	4.82	-1.66
31	214	-5	20.98	1.79	0.46	-8.01	3.73	4.53
32	98	-10	20.98	1.79	0.51	6.45	4.22	-6.02
33	171	-15	20.98	1.79	0.60	-4.53	5.05	5.63
34	78	-5	20.98	1.74	0.50	7.36	3.91	3.23
35	126	-10	20.98	1.74	0.59	-4.06	4.77	6.28
36	225	-15	20.98	1.74	0.64	3.82	5.32	-2.80

where N_ω is the weight number of adjustable neurons in BP network, α is a random number less than 1, and ω_i is the weight of neurons at the current network layer.

Including the above modification of the network evaluation function, the improved algorithm flow is shown in Figure 6. Taking the 600 algorithm iterations of the same complexity as an example, the efficiency comparison between the traditional BP algorithm and the improved fuzzy random BP algorithm is shown in Figure 7. It can be seen that the response of the new network is smoother than that of the traditional network. In addition, the new network has smaller weights and biases, which greatly reduces overfitting.

4. Fuzzy Random BP Network Prediction Model for Frost Heave Characteristics

4.1. Determination of Input and Output. The practice of underground freezing engineering shows that the frost heave characteristics under the action of tidal flow have obvious uncertainty. Combined with the previous tests on frost heave characteristics, it was found that both frost

Table 4: Engineering prediction results of frost heave characteristics.

Serial number	Input parameters: Tidal flow peak value (cm)	Freezing temperature (°C)	Moisture content (%)	Dry density (g/cm^3)	Compare the predicted and measured values: Frost heaving force (MPa)	Error of frost heaving force (%)	Frost heaving rate (%)	Error of frost heave rate (%)
1	81	-5	19.13	1.55	0.36	4.40	4.40	5.15
2	96	-10	19.13	1.55	0.43	-4.78	4.68	3.61
3	137	-15	19.13	1.55	0.52	6.64	6.42	-4.50
4	99	-5	23.19	1.50	0.41	-5.15	5.13	5.33
5	228	-10	23.19	1.50	0.48	5.37	5.68	6.31
6	180	-15	23.19	1.50	0.59	-6.49	6.38	-7.88
7	122	-5	16.28	1.64	0.27	-2.87	2.82	4.23
8	150	-10	16.28	1.64	0.37	4.18	4.08	5.31
9	254	-15	16.28	1.64	0.43	-4.40	4.88	-6.50
10	115	-5	17.92	1.59	0.33	3.54	3.32	4.24
11	204	-10	17.92	1.59	0.39	3.93	4.17	5.44
12	301	-15	17.92	1.59	0.49	-4.83	4.57	-3.16
13	173	-5	20.25	1.52	0.38	3.57	3.37	5.05
14	112	-10	20.25	1.52	0.46	4.07	3.89	4.89
15	184	-15	20.25	1.52	0.56	-4.83	4.72	-5.91
16	130	-5	24.61	1.44	0.42	3.51	3.88	6.15
17	112	-10	24.61	1.44	0.49	3.98	4.33	-4.03
18	207	-15	24.61	1.44	0.60	5.60	5.36	5.57
19	74	-5	21.94	1.48	0.39	4.12	3.77	4.18
20	116	-10	21.94	1.48	0.47	-7.09	4.32	-6.32
21	174	-15	21.94	1.48	0.57	3.46	5.29	3.98

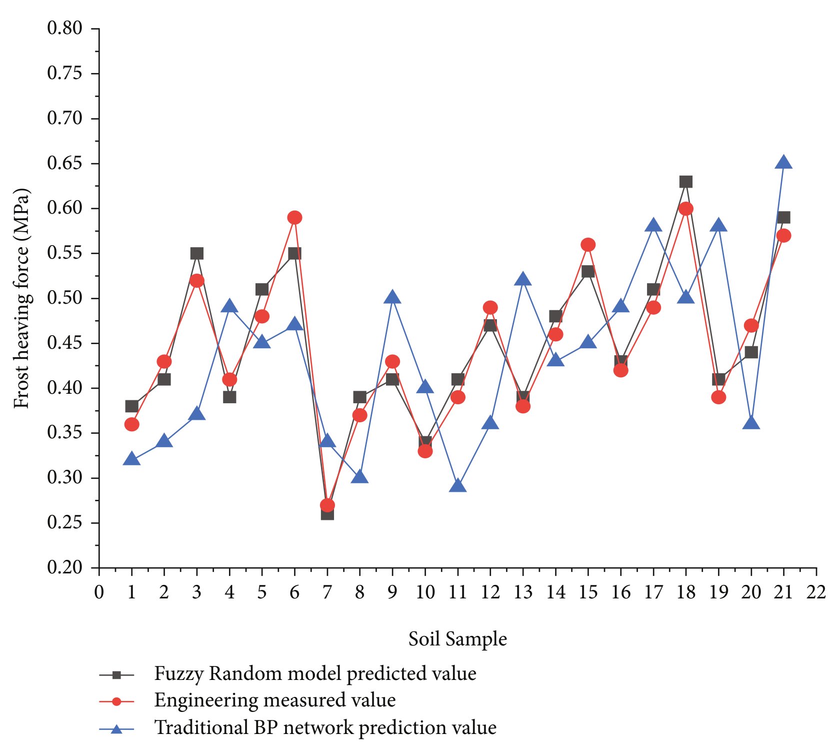

Figure 8: Comparison of fuzzy random model predicted and measured values of frost heaving force.

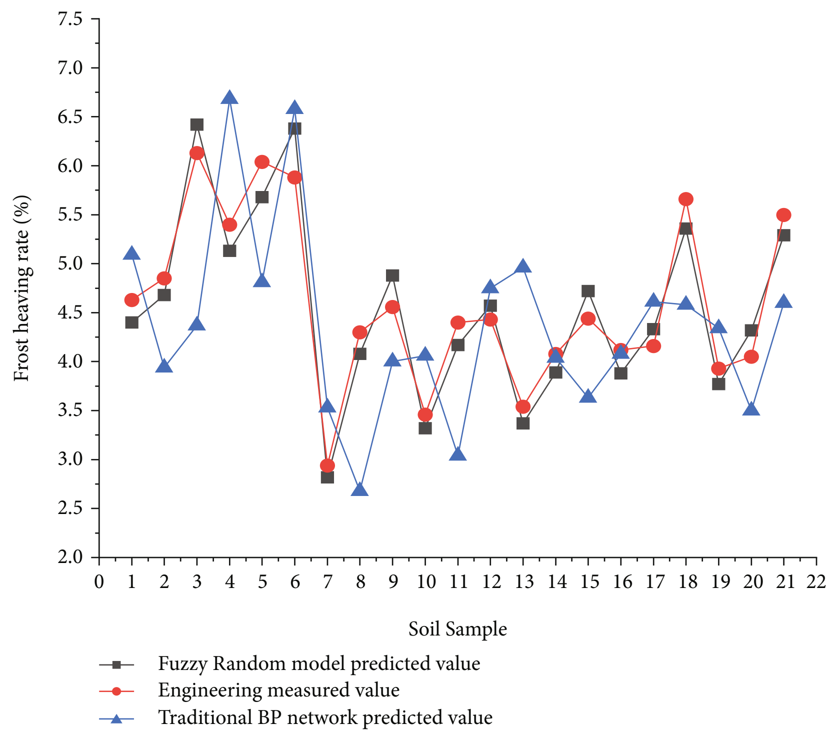

FIGURE 9: Comparison of fuzzy random model predicted and measured values of frost heaving rate.

heaving force and rate produced fuzzy random distributions under the comprehensive action of different tidal flow peak value, freezing temperature, natural water content, and dry density, so the above four parameters were used as the input of the fuzzy random BP network for predicting frost heave characteristics [25, 26].

In this study, the frost heaving force and rate of frozen soil were tested; the purpose of which was to master the frost heaving law of the construction layer of metro contact passage and to prevent safety accidents caused by tunnel position deviation and segment damage. To simplify the model, the frost heaving rate force and rate were taken as the output of the prediction model of frost heave characteristics of the fuzzy random BP network.

4.2. Determination of Hidden Layer Elements. In a BP neural network, it is also very important to select the number of hidden layer elements. If the number of hidden elements is too small, the whole network cannot train samples and process information well. If the number is too large, it will directly lead to structural redundancy and local minimum. To balance the relationship between them, the following formula is usually used to determine the number of hidden units in the prediction network model [27, 28].

$$Z = \sqrt{mn + 1.68n + 0.93}, \tag{9}$$

where Z is the number of hidden layer units, n is the number of inputs for the network, and m is the number of outputs for the network.

Substituting the number of inputs and outputs of this prediction model into Equation (9), Z was equal to 3.96. Therefore, the number of hidden layer elements in the prediction model for frost heave characteristics of fuzzy random BP network was set as 4.

4.3. Training of Fuzzy Random BP Network Prediction Model. In order to effectively train the fuzzy random BP network and make the prediction model accurately simulate the frost heave characteristics of underground frozen soil, the frozen soil parameters of the contact passages between different stations of Nantong metro line 1 were selected as the training samples of the model. The network took the peak value of tidal flow, freezing temperature, moisture content, and dry density as inputs and the frost heaving force and rate as outputs. According to the algorithm principle of the improved fuzzy random BP neural network, sufficient sample data were used for training, and the condition of terminating learning ε was set to e^{-6}. The initial value of ms w was 4.5, $\gamma = 0.68$, $\alpha = 0.7$, $N_\omega = 6$, $\omega_1 = 4.5$, $\omega_2 = 3.2$, $\omega_3 = 5.4$, $\omega_4 = 2.9$, $\omega_5 = 8.3$, and $\omega_6 = 1.8$. The training set P was 150, and the training sample error was controlled within 10% [29, 30]. Results of the network training are shown in Table 3.

With the focus on improving the fuzzy random BP network prediction model, the frost heave characteristics of frozen soil samples in the Nantong metro tunnel were used for training. The results show that the error of frost heaving force and rate is less than the training error when considering the tidal current peak value, freezing temperature, natural water content, and dry density. Therefore, the network prediction model in the study can better identify the frost heave characteristics of the horizontal frozen clay layer in the Nantong metro and effectively reflect the frost heaving uncertainty in underground freezing engineering.

5. Engineering Example for Checking Calculation

In order to further verify the applicability of the fuzzy random BP network prediction model for frost heave characteristics, the freezing condition of the underground clay layer in Nantong metro line 2 was selected as a validation example. The frost heaving force and rate under different tidal flow peak values, freezing temperature, natural water content, and dry density were compared with the measured values [31]. The results are shown in Table 4.

It can be seen from the results in Figures 8 and 9 that the fuzzy random BP network prediction model can make the predicted values of frost heaving force and rate basically coincide with the measured values under different working conditions, and the error is less than 8%. Compared with the traditional BP network model, the prediction error is reduced by 7%. Therefore, this prediction model can be used as an effective tool to predict the horizontal frost heaving characteristics during the freezing method construction of Nantong metro contact passage.

6. Conclusions

(1) The frost heaving test of the clay layer in the metro contact passage shows that the frost heave characteristics of clay are influenced by tidal current, freezing temperature, natural water content, and dry density, and the change rules are different. According to the frost heaving curve, the frost heaving force and rate of the same soil layer increase with the decrease of freezing temperature. In addition, due to the comprehensive influence of freezing temperature, natural water content, dry density, and tidal current peak, the frost heave characteristics of different soil samples are obviously uncertain

(2) With the goal of improving the deficiency of the traditional BP neural network algorithm in solving random engineering problems, random factors and mean square error between layers were used to modify the evaluation function of the network model. On this basis, the peak values of tidal flow, freezing temperature, natural water content, and dry density were taken as input values, the frost heaving force and rate of frozen soil were taken as output values, the number of middle hidden layer elements was set as 4, and an improved prediction model of frost heave characteristics of fuzzy random BP network was established. The new network prediction model has better weights and smaller biases, and its response tends to be smoother than that of the traditional network, which greatly reduces the phenomenon of overfitting

(3) The engineering example shows that the improved BP neural network prediction model can make the predicted value of frost heaving force and rate basically coincide with the measured value under different working conditions, and the error is controlled within 8% after effective training. Therefore, the prediction model can be used as an effective tool for the prediction of frost heave characteristics in Nantong metro freezing construction, and the corresponding model and method can also be extended to similar engineering cases

Data Availability

All data, models, and codes appeared in the submitted article.

Conflicts of Interest

The authors declare that they have no conflicts of interest.

Acknowledgments

We express our sincere thanks to Chief Engineers Zhou Xia and Zhou Feng and to Dr. Lin Jian for their enthusiastic support in providing related information. This work was supported by the Nantong Municipal Science and Technology Program of China (grant number MS12021028), the Innovation and Entrepreneurship Training Program for University Students in Jiangsu Province of China (grant number 202111052016Y), and the "Qinglan Project" for Training of University Teachers in Jiangsu Province of China.

References

[1] Y. Yang, Y. Lai, and X. Chang, "Experimental and theoretical studies on the creep behavior of warm ice-rich frozen sand," *Cold Regions Science and Technology*, vol. 63, no. 1-2, pp. 61–67, 2010.

[2] Q. Miao, F. Niu, Z. Lin, J. Luo, and M. Liu, "Comparing frost heave characteristics in cut and embankment sections along a high-speed railway in seasonally frozen ground of Northeast China," *Cold Regions Science and Technology*, vol. 170, article 102921, 2020.

[3] H. Jihui, X. Caichu, and H. Changling, "Distribution form and simplified calculation method of frost heaving force load in highway tunnel in cold region," *Modern Tunnelling Technology*, vol. 53, no. 5, pp. 63–70, 2016.

[4] Y. Lu, X. Li, and A. Chan, "Damage constitutive model of single flaw sandstone under freeze-thaw and load," *Cold Regions Science and Technology*, vol. 159, pp. 20–28, 2019.

[5] X. Lu, F. Zhang, W. Qin, H. Zheng, and D. Feng, "Experimental investigation on frost heave characteristics of saturated clay soil under different stress levels and temperature gradients," *Cold Regions Science and Technology*, vol. 192, article 103379, 2021.

[6] Y. Zhu, Y. Li, Z. Hao, L. Luo, J. Luo, and L. Wang, "An analytical solution for the frost heaving force and displacement of a noncircular tunnel," *Computers and Geotechnics*, vol. 133, article 104022, 2021.

[7] J. Zhou, W. Zhao, and Y. Tang, "Practical prediction method on frost heave of soft clay in artificial ground freezing with field experiment," *Tunnelling and Underground Space Technology*, vol. 107, article 103647, 2021.

[8] H. Liu, P. Maghoul, A. Shalaby, and A. Bahari, "Thermo-hydro-mechanical modeling of frost heave using the theory of poroelasticity for frost-susceptible soils in double-barrel culvert sites," *Transportation Geotechnics*, vol. 20, article 100251, 2019.

[9] J. Luo, L. Tang, X. Ling, and L. Geng, "Experimental and analytical investigation on frost heave characteristics of an unsaturated moderately expansive clay," *Cold Regions Science and Technology*, vol. 155, pp. 343–353, 2018.

[10] X. Zhang, M. Zhang, W. Pei, and J. Lu, "Experimental study of the hydro-thermal characteristics and frost heave behavior of a saturated silt within a closed freezing system," *Applied Thermal Engineering*, vol. 129, pp. 1447–1454, 2018.

[11] M. Zhelnin, A. Kostina, A. Prokhorov, O. Plekhov, M. Semin, and L. Levin, "Coupled thermo-hydro-mechanical modeling of frost heave and water migration during artificial freezing of soils for mineshaft sinking," *Journal of Rock Mechanics and Geotechnical Engineering*, 2021.

[12] J. Chen, A. Li, C. Bao et al., "A deep learning forecasting method for frost heave deformation of high-speed railway subgrade," *Cold Regions Science and Technology*, vol. 185, article 103265, 2021.

[13] C. Amanuma, T. Kanauchi, S. Akagawa, Z. Hao, and S. Kanie, "Evaluation of frost heave pressure characteristics in transverse direction to heat flow," *Procedia Engineering*, vol. 171, pp. 461–468, 2017.

[14] S. Ponti, N. Cannone, and M. Guglielmin, "Needle ice formation, induced frost heave, and frost creep: a case study through photogrammetry at Stelvio Pass (Italian Central Alps)," *Catena*, vol. 164, pp. 62–70, 2018.

[15] H. Cai, Z. Liu, S. Li, and T. Zheng, "Improved analytical prediction of ground frost heave during tunnel construction using artificial ground freezing technique," *Tunnelling and Underground Space Technology*, vol. 92, article 103050, 2019.

[16] Y. Wang, Y. Liu, K. Yang, and P. Sun, "Numerical study of frost heave behavior in U-elbow of ground heat exchanger," *Computers and Geotechnics*, vol. 99, pp. 1–13, 2018.

[17] Y. Cui, H. Liu, Q. Wang et al., "Investigation on the ignition delay prediction model of multi-component surrogates based on back propagation (BP) neural network," *Combustion and Flame*, vol. 237, article 111852, 2022.

[18] J. Li, X. Yao, and K. Xu, "A comprehensive model integrating BP neural network and RSM for the prediction and optimization of syngas quality," *Biomass and Bioenergy*, vol. 155, article 106278, 2021.

[19] K. Gong, D.-D. He, S.-Y. Chen, S. W. Jing, and Y. L. Zheng, "BP neural network analysis for identification of explosive in package by tagged neutron method," *Nuclear Instruments and Methods in Physics Research Section A: Accelerators, Spectrometers, Detectors and Associated Equipment*, vol. 1017, article 165810, 2021.

[20] J. Qian, P. Wang, C. Pu, and G. Chen, "Joint application of multi-object beetle antennae search algorithm and BAS-BP fuel cost forecast network on optimal active power dispatch problems," *Knowledge-Based Systems*, vol. 226, article 107149, 2021.

[21] W. Shen, G. Li, X. Wei et al., "Assessment of dairy cow feed intake based on BP neural network with polynomial decay learning rate," *Information Processing in Agriculture*, vol. 8, 2021.

[22] D. Yao, Y.-c. Duan, M.-y. Li, and Y. P. Guan, "Hybrid identification method of coupled viscoplastic-damage constitutive parameters based on BP neural network and genetic algorithm," *Engineering Fracture Mechanics*, vol. 257, article 108027, 2021.

[23] L. Wang and X. Bi, "Risk assessment of knowledge fusion in an innovation ecosystem based on a GA- BP neural network," *Cognitive Systems Research*, vol. 66, pp. 201–210, 2021.

[24] H.-c. Liao, Y. Gao, Q.-g. Wang, and D. Wilson, "Development of viscosity model for aluminum alloys using BP neural network," *Transactions of Nonferrous Metals Society of China*, vol. 31, no. 10, pp. 2978–2985, 2021.

[25] Y. He, Z. Meng, H. Xu, and Y. Zou, "A dynamic model of evaluating differential automatic method for solving plane problems based on BP neural network algorithm," *Physica A: Statistical Mechanics and its Applications*, vol. 556, article 124845, 2020.

[26] G. Chen, B. Tang, X. Zeng, P. Zhou, P. Kang, and H. Long, "Short-term wind speed forecasting based on long short-term memory and improved BP neural network," *International Journal of Electrical Power & Energy Systems*, vol. 134, p. 107365, 2022.

[27] X. Zhang, D. Li, L. Chen, F. Ming, and Y. Liu, "A new integral model for predicting the hydraulic conductivity of saturated frozen soil," *Journal of Hydrology*, vol. 603, article 126838, 2021.

[28] H. Wang, Y. Zheng, W. Shi, and X. Wang, "Comparison of Arrhenius model and artificial neuronal network for predicting quality changes of frozen tilapia (Oreochromis niloticus)," *Food Chemistry*, vol. 372, article 131268, 2022.

[29] L. Chen and X. Zhang, "A model for predicting the hydraulic conductivity of warm saturated frozen soil," *Building and Environment*, vol. 179, article 106939, 2020.

[30] J. Ren and S. K. Vanapalli, "Empirical model for predicting the resilient modulus of frozen unbound road materials using a hyperbolic function," *Transportation Geotechnics*, vol. 17, pp. 66–74, 2018.

[31] Y. Alyousifi, M. Othman, A. Husin, and U. Rathnayake, "A new hybrid fuzzy time series model with an application to predict PM_{10} concentration," *Ecotoxicology and Environmental Safety*, vol. 227, article 112875, 2021.